

Platinum Priority – Prostate Cancer

Editorial by Ninghan Feng, Yu Yin, Yiping He and Jiaoti Huang on pp. 79–80 of this issue

SRRM4 Drives Neuroendocrine Transdifferentiation of Prostate Adenocarcinoma Under Androgen Receptor Pathway Inhibition

Yinan Li^{a,†}, Nilgun Donmez^{a,b,†}, Cenk Sahinalp^{a,b}, Ning Xie^a, Yuwei Wang^c, Hui Xue^c, Fan Mo^a, Himisha Beltran^d, Martin Gleave^a, Yuzhuo Wang^{a,c}, Colin Collins^{a,b,e,†,*}, Xuesen Dong^{a,†,*}

^a Vancouver Prostate Centre, Department of Urologic Sciences, University of British Columbia, Vancouver, Canada; ^b School of Computing Science, Simon Fraser University, Burnaby, Canada; ^c Department of Experimental Therapeutics, British Columbia Cancer Agency, Vancouver, Canada; ^d Department of Medicine, Weill Cornell Medicine, New York, NY, USA; ^e Laboratory for Advanced Genome Analysis, Vancouver, Canada

Article info

Article history:

Accepted April 20, 2016

Associate Editor:

James Catto

Keywords:

Neuroendocrine prostate cancer
AR inhibition
SRRM4
Alternative RNA splicing

Abstract

Background: Neuroendocrine prostate cancer (NEPC) is an aggressive subtype of castration-resistant prostate cancer that typically does not respond to androgen receptor pathway inhibition (ARPI), and its diagnosis is increasing.

Objective: To understand how NEPC develops and to identify driver genes to inform therapy for NEPC prevention.

Design, setting, and participants: Whole-transcriptome sequencing data were extracted from prostate tumors from two independent cohorts: The Beltran cohort contained 27 adenocarcinoma and five NEPC patient samples, and the Vancouver Prostate Centre cohort contained three patient samples and nine patient-derived xenografts.

Intervention: A novel bioinformatics tool, comparative alternative splicing detection (COMPAS), was invented to analyze alternative RNA splicing on RNA-sequencing data.

Outcome measurements and statistical analysis: COMPAS identified potential driver genes for NEPC development. Biochemical and biological validations were performed in both prostate cell and tumor models.

Results and limitation: More than 66% of the splice events were predicted to be regulated by the RNA splicing factor serine/arginine repetitive matrix 4 (SRRM4). In vitro and in vivo evidence confirmed that one SRRM4 target gene was the RE1 silencing transcription factor (*REST*), a master regulator of neurogenesis. Moreover, SRRM4 strongly stimulated adenocarcinoma cells to express NEPC biomarkers, and this effect was exacerbated by ARPI. ARPI combined with a gain of SRRM4-induced adenocarcinoma cells to assume multicellular spheroid morphology and was essential in establishing progressive NEPC xenografts. These SRRM4 actions were further enhanced by loss of function of *TP53*.

Conclusions: SRRM4 drives NEPC progression. This knowledge may guide the development of novel therapeutics aimed at NEPC.

Patient summary: Using next-generation RNA sequencing and our newly developed bioinformatics tool, we identified a neuroendocrine prostate cancer (NEPC)-specific RNA splicing signature that is predominantly controlled by serine/arginine repetitive matrix 4 (SRRM4). We confirmed that SRRM4 drives NEPC progression, and we propose SRRM4 as a potential therapeutic target for NEPC.

© 2016 European Association of Urology. Published by Elsevier B.V. All rights reserved.

[†] These authors contributed equally to this manuscript.

[‡] Co-senior authors.

* Corresponding authors. Vancouver Prostate Centre, Department of Urologic Sciences, University of British Columbia, 2660 Oak Street, Vancouver, British Columbia, V6H 3Z6, Canada.

Tel. +1 604 875 4111; Fax: +1 604 875 5654.

E-mail addresses: ccollins@prostatecentre.com (C. Collins), xdong@prostatecentre.com (X. Dong).

1. Introduction

Next-generation androgen receptor (AR) pathway inhibitors that suppress AR signaling in castration-resistant prostate cancers (CRPCs) have improved patient outcomes [1]; however, emerging evidence suggests that lethal neuroendocrine prostate cancer (NEPC) becomes more prevalent in patients treated with first- or second-line AR pathway inhibitors [2,3]. NEPC cells lose their granular structure and present small cell neuroendocrine-like morphology [4]. They express typical neuroendocrine markers such as chromogranins, synaptophysin (SYP), and neurospecific enolase (NSE) but no or low levels of AR and AR-regulated genes [5–8]. Because AR signaling is required for epithelial cell differentiation during prostate development, AR pathway inhibition (ARPI) likely triggers developmental reprogramming of adenocarcinoma prostate cancer (AdPC) to NEPC through a transdifferentiation mechanism [8]. Although ARPI improves overall survival for men with metastatic CRPC, it may result in treatment-induced progression to NEPC as a resistance mechanism; NEPC is insensitive to ARPI therapy.

RNA sequencing (RNA-seq) can elucidate molecular mechanisms of NEPC development [4,7]. Although recent work has focused on identifying the genomic and transcriptomic profiles of NEPC, analyses of alternative splicing (AS) have lagged. Access to RNA-seq data from independent (Vancouver Prostate Centre [VPC] and Beltran) cohorts allowed us to decipher NEPC-specific AS signatures. The VPC cohort contained three patient samples and nine patient-derived xenografts (PDXs) [6]. These PDX models had remarkable fidelity with respect to genome, transcriptome, and responses to ARPI in relation to the patient tumors [6]. The Beltran cohort contained clinical samples from 27 AdPC and 5 NEPC patients [4]. Together, these cohorts generated an RNA-seq data set for analyzing NEPC-specific AS signatures.

Although the expression of several genes is correlated with NEPC [4,7–9], none were confirmed as driving NEPC transdifferentiation. We reported loss of RE1 silencing transcription factor (*REST*) in NEPC [7,10]. *REST* is highly expressed in embryonic stem cells and non-neuronal cells. It acts as a negative master regulator of neurogenesis by suppressing genes required for neural cell differentiation [11]. One mechanism for cells to compromise *REST* function during neural differentiation is AS of *REST* into REST4 [12]. A neural-specific exon (exon N) becomes inserted between exons 3 and 4, resulting in translation of a truncated and functionally reprogrammed REST4 protein. These findings indicate that although transcriptomic studies can identify genes such as *REST* associated with NEPC progression, analyzing NEPC-specific AS signatures to identify RNA splice factors may lead to unrecognized mechanisms of NEPC progression and novel therapeutic approaches. Loss of function of *RB1* and *TP53* genes as well as gain of function of *AURKA* were also reported in NEPC [4,9,13]. These genes are known as cell cycle regulators. Whether they can confer cancer cells with an NEPC phenotype and drive NEPC transdifferentiation has not been established.

In this study, we developed a computational tool, COMPAS, to identify an NEPC-specific AS signature of the genes that are predominantly spliced by SRRM4. Molecular and biological evidence validated these findings and demonstrated that, in the context of ARPI, SRRM4 can drive transdifferentiation to NEPC.

2. Methods

Whole-transcriptome sequencing data were extracted from prostate tumors from two independent (VPC and Beltran) cohorts to develop and validate the COMPAS tool. Details are provided in Supplement 1.

3. Results

3.1. COMPAS identifies a neuroendocrine prostate cancer-specific alternative splicing signature

In the VPC cohort, 1639 genes were differentially expressed (Benjamini-Hochberg corrected, false discovery rate [FDR] <0.01) between NEPC and AdPC samples (Fig. 1a, Supplementary Fig. 1, and Supplementary Table 1a and 1b). The NEPC samples also exhibited distinct AS profiles (Fig. 1b and 1c). Among 1036 AS events from 916 genes predicted by COMPAS, 106 events showed statistically significant differences between NEPC and AdPC samples (Benjamini-Hochberg corrected, FDR <0.01) (Supplementary Table 1c and 1d). Most AS events occurred in distinct genes. The exceptions were the *VAV2* and *CADPS2* genes, which harbored two distinct (nonoverlapping) cassette exon inclusion events.

In the Beltran cohort, 1549 genes were differentially expressed between AdPC and NEPC samples (Supplementary Fig. 1 and 2a and Supplementary Table 1e and 1f). Among the 1023 AS events from the 889 genes predicted, 59 AS events showed statistically significant differences (Benjamini-Hochberg corrected, FDR <0.01) (Supplementary Fig. 2b and 2c and Supplementary Table 1g and 1h). This cohort was sequenced to significantly lower read depth than the VPC cohort; therefore, our power to detect AS was reduced for low abundance transcripts. Two tumors from this cohort were also diagnosed as “prostate cancer with neuroendocrine differentiation,” indicating mixed phenotypes. In contrast to the VPC cohort, the Beltran cohort did not exhibit significant differential expression of *AR* and *CHGA* in any NEPC samples (Supplementary Fig. 3a and 3b).

3.2. Common neuroendocrine prostate cancer-specific alternative splicing signature between Vancouver Prostate Centre and Beltran cohorts

The VPC and Beltran cohorts shared 24 NEPC-specific AS events (Supplementary Table 2a). Although the majority of these events featured a single exon inclusion in NEPC, some AS events such as those in *PDGFA* and *MYO6* involved multiple exons and/or alternative C-terminal sequences. Gene ontology (GO) analysis of these genes revealed

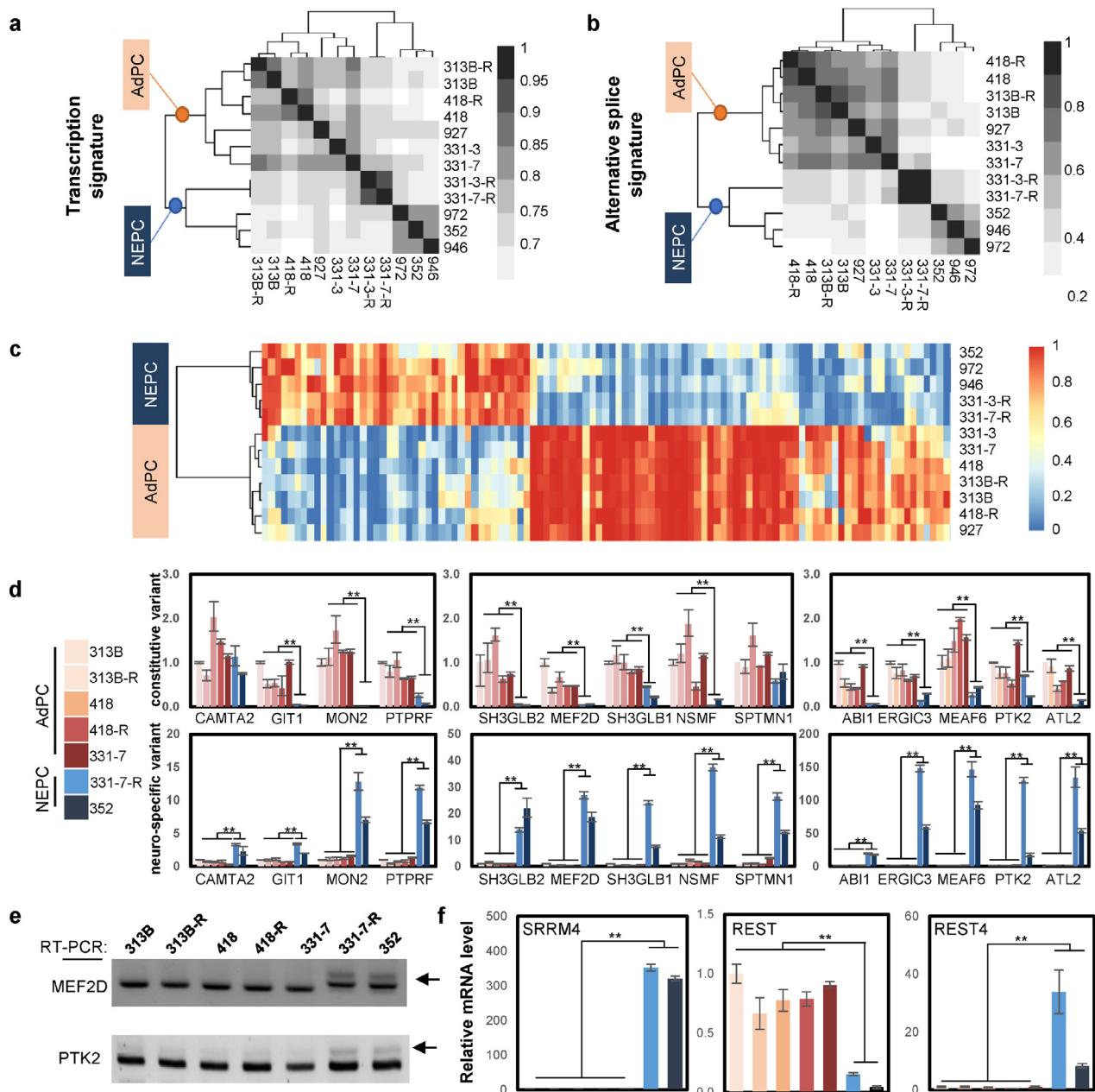


Fig. 1 – COMPAS identifies a neuroendocrine prostate cancer (NEPC)-specific signature in prostate tumor biopsies. (a) A heat map shows Spearman correlation values using normalized gene expression of the samples from the Vancouver Prostate Centre (VPC) cohort. Unsupervised hierarchical clustering was performed using the *heatmap* package in R, based on the entire set of genes detected (55 227 genes). (b) A heat map shows Spearman correlation values using the splicing index of samples from the VPC cohort. Clustering is performed as in panel (a), based on the entire set of splicing predictions (1035 alternative splicing [AS] events). (c) NEPC-specific AS signatures are generated based on 106 differential AS events from 104 genes between NEPC and AdPC samples from the VPC cohort (Benjamini-Hochberg corrected, FDR < 0.01). (d) Total RNA was extracted from adenocarcinoma prostate cancer and NEPC tumor samples. Real-time polymerase chain reaction (PCR) measured relative messenger RNA (mRNA) levels of the constitutive and NEPC-specific variants of SRRM4-regulated genes predicted by COMPAS. (e) Predicted AS events regulated by SRRM4 in patient-derived xenografts were also validated by RT-PCR followed by Sanger sequencing. (f) Real-time PCR measured mRNA levels of SRRM4, REST and REST4 in tumor samples from the VPC cohort. Results were presented as mean plus or minus standard deviation. ** $p < 0.01$. AdPC = adenocarcinoma prostate cancer; mRNA = messenger RNA; NEPC = neuroendocrine prostate cancer; RT-PCR = reverse transcription polymerase chain reaction.

biological processes including cell surface receptor-linked signal transduction, vesicle-mediated and intracellular transport, and secretion and establishment of cellular localization. Cellular component GO terms were enriched in the leading edge, cell projection, and cytoskeleton, suggesting these genes may regulate cell morphology (FDR

<0.05) (Supplementary Table 2b). None of these 24 genes exhibited a significant change in overall expression between NEPC and AdPC samples (Supplementary Fig. 4a), emphasizing the complementary role of AS in transcription regulation during NEPC transdifferentiation. We selected 14 AS events from the 24-gene signature

predicted by COMPAS and successfully validated all of them in tumors and cells overexpressing SRRM4 (Fig. 1d and 1e and Supplementary Fig. 5).

Although the functions of these NEPC splice variants are mostly unknown, 16 of these genes were reported to be regulated by the splicing factor SRRM4 in N2A neuroblastoma and 293T embryonic kidney cell lines [12]. Comparing their results with our VPC and Beltran NEPC signatures separately, we obtained even higher rates of overlap (36 and 21 in the VPC and Beltran cohorts, respectively) (Supplementary Table 2c). Moreover, several genes from our AS signature were also reported in Bronx Waltzer mice carrying mutant *SRRM4* [14]. *SRRM4* is one of the most significantly upregulated genes in NEPC in both the VPC and Beltran cohorts, and its levels are negatively associated with *REST* expression ($p < 0.001$) (Fig. 1f and Supplementary Fig. 4b and 4c). These findings suggest a possible role for SRRM4 in driving NEPC transdifferentiation through regulating *REST* splicing. AS of *REST* was not identified by COMPAS,

likely due to the low abundance of *REST* expression in NEPC samples that prevented COMPAS from calling it.

3.3. *SRRM4* is an upstream regulator of *REST* gene functions in prostate cancer cells

Using multiple cell models, we showed that NCI-H660 (NEPC line) and VCaP cells express elevated levels of SRRM4 and REST4 proteins and low levels of REST protein (Fig. 2a). Consistently, these cells expressed enhanced REST4 messenger RNA (mRNA) levels but extremely low levels of REST (Fig. 2b). These results were consistent with those from NEPC tumor samples (Fig. 1f and Supplementary Fig. 4b and 4c), in which elevated SRRM4 expression was negatively associated with the expression ratio of REST:REST4.

To determine whether SRRM4 regulated *REST* expression, we overexpressed SRRM4 in LNCaP cells (Fig. 2c). There was a 30% decrease in REST but a 130-fold increase in REST4 mRNA levels. SRRM4 depletion in VCaP cells resulted

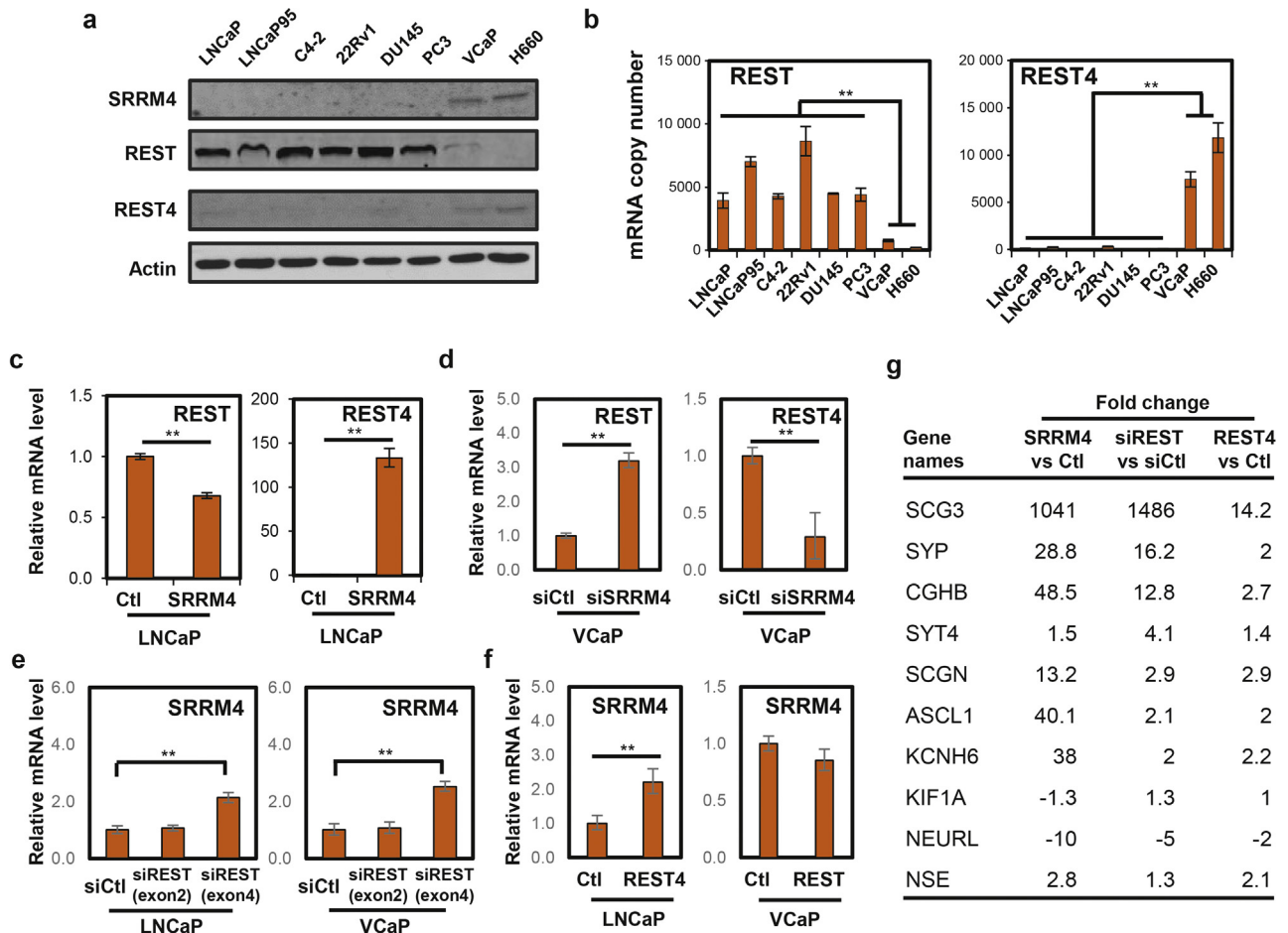


Fig. 2 – SRRM4 is an upstream regulator of *REST*. Prostate cancer cell lines were cultured in medium, as described in the materials and methods (Supplement 1). Total RNA and protein lysates were collected for immunoblotting (a) and real-time polymerase chain reaction (PCR) assays (b). (c) LNCaP cells were transfected with control or SRRM4 expression vector. (d) VCaP cells were transfected with control or SRRM4 small interfering RNA (siRNA) for 48 h. Total RNA was collected and used to measure REST and REST4 mRNA levels by real-time PCR. (e) LNCaP and VCaP cells were transfected with control or REST siRNAs against exon 2 or exon 4. (f) LNCaP or VCaP cells were transfected with control, REST4, or REST plasmid. Total RNA was collected and used to measure SRRM4 messenger RNA (mRNA) levels. The results were presented as mean plus or minus standard deviation. ** $p < 0.01$. (g) LNCaP cells were transfected with control or SRRM4 expression vector (left panel), control or REST siRNA (middle panel), or control or REST4 expression vector (right panel). Total RNA was collected and used to measure mRNA levels of neuroendocrine prostate cancer biomarkers using real-time PCR. Ctl = control; mRNA = messenger RNA; si = small interfering.

in a 10-fold increase in REST and a 90% decrease in REST4 mRNA levels (Fig. 2d). Consistent REST and REST4 protein expression regulated by SRRM4 was also confirmed (Supplementary Fig. 6a and 6b). To determine whether REST regulated SRRM4 expression, two small interfering RNAs (siRNAs) were used to deplete REST. The exon 2 siRNA depleted REST and REST4 expression (Supplementary Fig. 6c and 6d). Exon 4 siRNA depleted REST but induced a 50-fold increase of REST4. Regardless, minor changes of SRRM4 mRNA and no change of SRRM4 protein levels were observed (Fig. 2e and Supplementary Fig. 6d). Overexpression of REST4, but not REST, caused a twofold increase in SRRM4 mRNA levels and no change in SRRM4 protein levels (Fig. 2f and Supplementary Fig. 6e and 6f). Gain of function

of SRRM4 and loss of function of REST resulted in a similar induction of NEPC biomarkers (Fig. 2g); however, SRRM4 exerted stronger effects. REST4 did not significantly alter the expression of NEPC biomarkers. These results suggest that a key mechanism through which SRRM4 induces the NEPC phenotype is reprogramming of REST function by AS and that SRRM4 is an upstream negative regulator of REST function.

3.4. Molecular mechanisms through which SRRM4 regulates alternative splicing of REST

RNA chromatin immunoprecipitation showed that SRRM4 recognized the region near the 3' splice site of REST intron 3

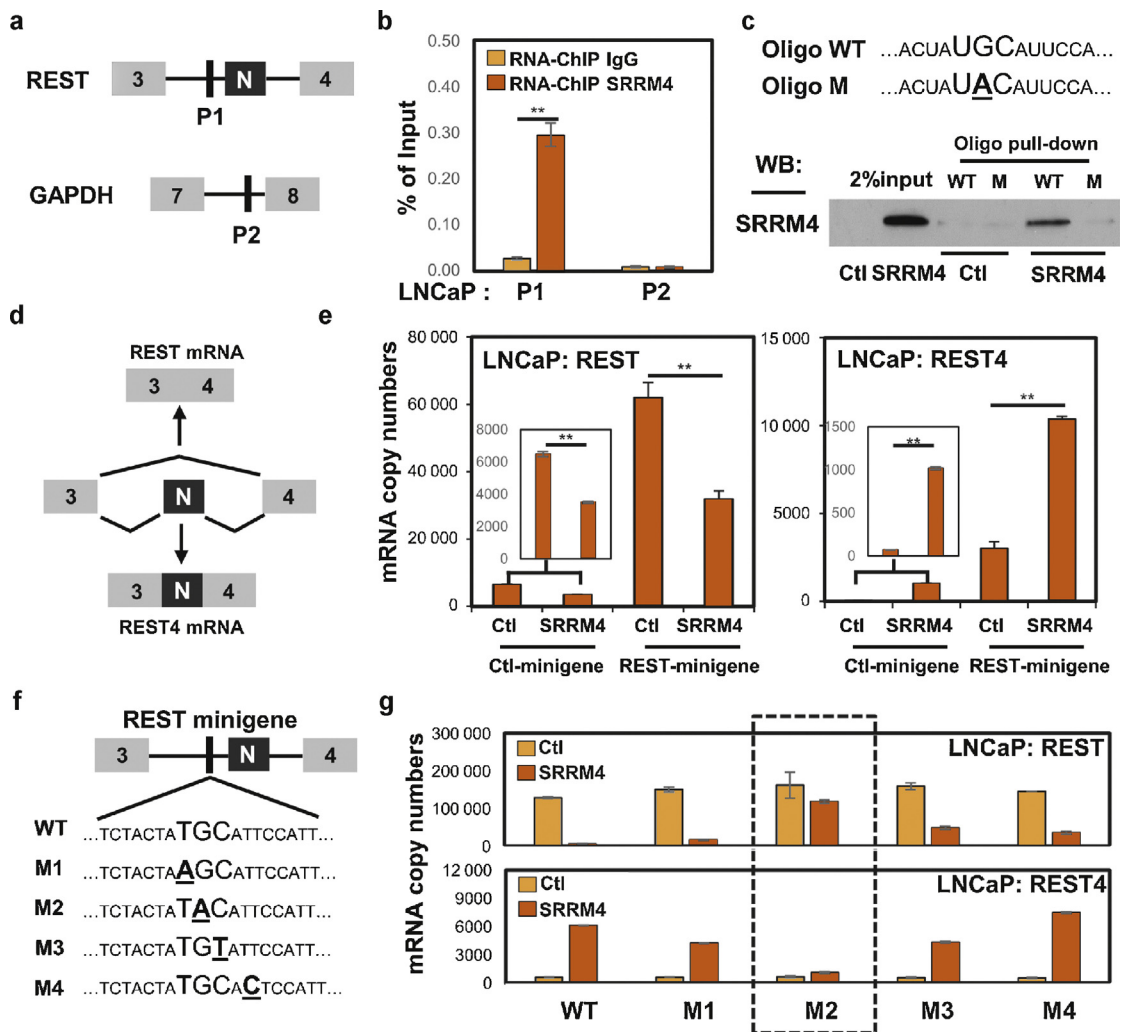


Fig. 3 – SRRM4 regulates alternative splicing (AS) of REST in prostate cancer cells. (a) A schematic diagram shows the regions (P1, P2) that were amplified in RNA chromatin immunoprecipitation (ChIP) assays. (b) LNCaP cells were transfected with Flag-SRRM4 plasmids. RNA-ChIP assays were performed using Flag antibody or control immunoglobulin G. Eluted RNA fragments were used as templates for real-time polymerase chain reaction (PCR). Signals were calculated as percentage of input. (c) Flag-tagged SRRM4 was purified from LNCaP cells to perform RNA pull-down assays. Oligo-associated proteins were detected by immunoblotting. (d) A schematic diagram shows the REST minigene structure and the AS variants derived from the minigene. (e) LNCaP cells were transfected with control or REST minigene reporter in the presence of $-/+$ SRRM4. Total RNA was extracted to measure REST and REST4 messenger RNA (mRNA) levels by real-time PCR. (f) Site-directed mutagenesis was performed around the UGC motif in the REST minigene. (g) LNCaP cells were transfected with control, REST minigene, or REST minigene with M1–M4 mutations in the presence of $-/+$ SRRM4. Total RNA was collected and used to measure REST and REST4 mRNA levels by real-time PCR. All results were derived from two independent experiments that were performed in triplicate. Data are presented as mean plus or minus standard deviation. ** $p < 0.01$ compared with controls. ChIP = chromatin immunoprecipitation; Ctl = control; M = mutation; mRNA = messenger RNA; WT = wild type; $-/+$ = transfected with control or expression vector of indicated genes.

(designated as the P1 region) (Fig. 3a and 3b). In contrast, SRRM4 enrichment to the control intron region (designated as P2) was extremely low (<0.01% in Fig. 3b and Supplementary Fig. 7a). It has been reported that the UGC motif is predicted to be a consensus SRRM4 recognition site near RNA splicing sites [15]. RNA pulldown assays confirmed that purified SRRM4 protein from LNCaP or 293T cells interacted directly with a UGC motif in *REST* intron 3 (Fig. 3c and Supplementary Fig. 7b). A *REST* minigene was constructed in which the exon N and its flanking approximately 300-base pair nucleotides were inserted in between exon 3 and 4 of the *REST* gene (Fig. 3d). This minigene is similar to the endogenous *REST* gene with respect to its response to SRRM4 overexpression (Fig. 3e and Supplementary Fig. 7c). Site-directed mutagenesis of all sites (M1–M4) around the UGC motif in the P1 region (Fig. 3f) indicated SRRM4-mediated exon N inclusion relied on the G within the UGC motif (Fig. 3g and Supplementary Fig. 7d). These results demonstrated that SRRM4 binds the UGC motif and induces exon N inclusion for *REST4* splicing.

3.5. AR pathway inhibition enhances SRRM4 to induce the neuroendocrine prostate cancer phenotype in prostate cancer cells

To study interactions between SRRM4 and ARPI, LNCaP and VCaP cells were cultured in androgen depletion medium and treated with dihydrotestosterone (DHT) or enzalutamide. AR inhibition did not alter *REST*, *REST4*, or *SRRM4* mRNA levels (Fig. 4a) but reduced *REST* protein expression (Fig. 4b). These results indicated that ARPI reduced *REST* post-transcriptionally, as reported [10]. Overexpression of SRRM4 by lentivirus induced the NEPC phenotype, and it became stronger with enzalutamide (Fig. 4c). These results together indicate that SRRM4 and ARPI target AS and protein expression of the *REST* gene, respectively, and that contributes additively to NEPC transdifferentiation.

3.6. RB1 and TP53 loss of function enhance SRRM4-induced neuroendocrine prostate cancer transdifferentiation

We depleted *RB1* or *TP53* by shRNA in LNCaP cells and then introduced exogenous SRRM4 by lentivirus (Supplementary

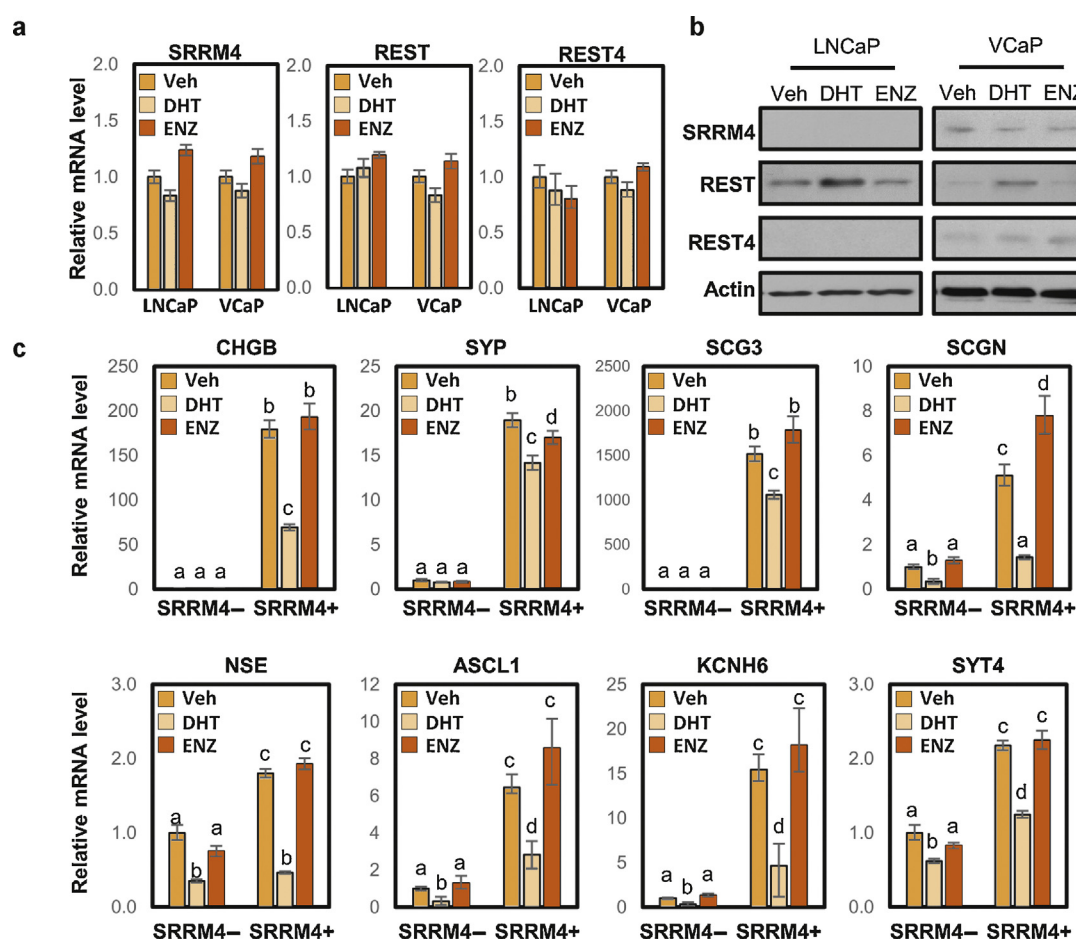


Fig. 4 – Androgen receptor pathway inhibition enhances SRRM4 actions to induce the neuroendocrine prostate cancer (NEPC) phenotype. LNCaP and VCaP cells (a and b) or LNCaP (control) and LNCaP (SRRM4) cells (c) were cultured in medium containing 10% charcoal-stripped serum for 48 h before being treated with vehicle, dihydrotestosterone, or enzalutamide. (a) Total RNA and protein lysates were collected. SRRM4, REST, and REST4 messenger RNA (mRNA) levels were detected by real-time polymerase chain reaction (PCR). (b) SRRM4, REST, REST4, and actin protein levels were detected by immunoblotting. (c) NEPC biomarker expression in mRNA was measured by real-time PCR. All results were presented as mean plus or minus standard deviation ($n = 3$; values without a common letter are significantly different, $p < 0.05$). These data were analyzed by one-way analysis of variance, followed by Tukey's multiple comparison tests. DHT = dihydrotestosterone; ENZ = enzalutamide; mRNA = messenger RNA; Veh = vehicle.

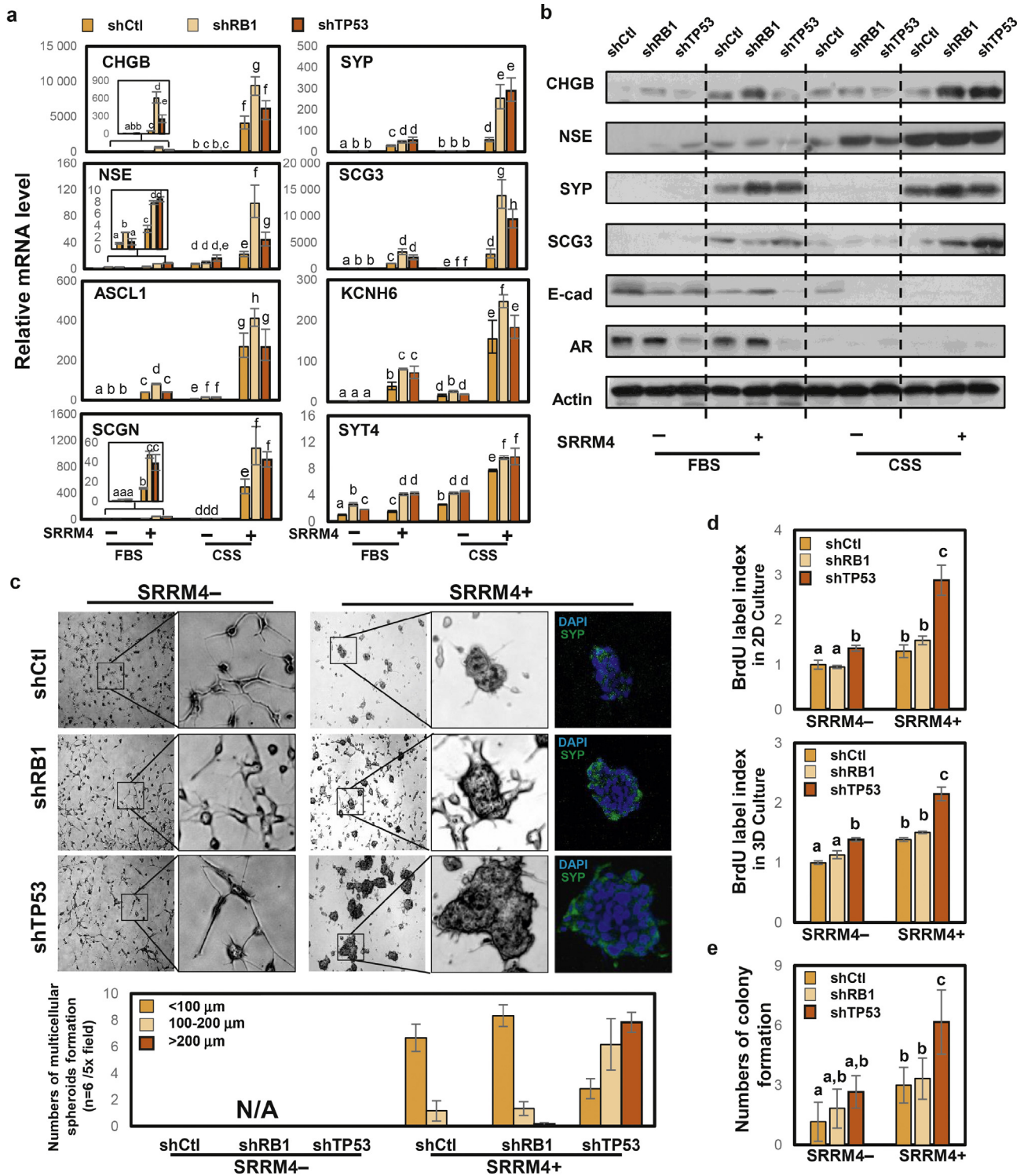


Fig. 5 – Roles of *TP53* and *RB1* depletion in SRRM4-induced neuroendocrine prostate cancer (NEPC) phenotype. LNCaP(SRRM4^{-/-}/shCtl), LNCaP(SRRM4^{+/+}/shCtl), LNCaP(SRRM4^{-/-}/shRB1), LNCaP(SRRM4^{+/+}/shRB1), LNCaP(SRRM4^{-/-}/shTP53), and LNCaP(SRRM4^{+/+}/shTP53) cells were cultured in RPMI 1640 medium containing either 10% fetal bovine serum or 10% charcoal-stripped serum (CSS) for 4 wk. Total RNA and protein lysates were collected and used to measure NEPC biomarker expression by real-time polymerase chain reaction (a) and by immunoblotting (b). (c) LNCaP cells with ^{-/-}SRRM4, ^{-/-}shRB1, or shTP53 were cultured in medium containing 10% CSS for 4 wk. Spheroids were fixed, immunostained with SYP antibody, and examined by fluorescence microscope. Multicellular spheroid formation was counted in both numbers and sizes per ×5 field. (d) LNCaP cells with ^{-/-}SRRM4, ^{-/-}shRB1 or shTP53 were cultured in medium containing 10% CSS in six-well plates (two-dimensional) or in collagen-embedded three-dimensional conditions. BrdU incorporation rates were calculated as described in the materials and methods (Supplement 1). (e) Colony formation assays were performed on LNCaP cells with ^{-/-}SRRM4, as indicated. Colonies were stained with crystal violet, and colony numbers were counted. All results are presented as mean plus or minus standard deviation (*n* = 3; values without a common letter are significantly different, *p* < 0.05). These data were analyzed by one-way analysis of variance followed by Tukey's multiple comparison tests. 2D = two-dimensional; 3D = three-dimensional; CSS = charcoal-stripped serum; DAPI = 4',6-diamidino-2-phenylindole; FBS = fetal bovine serum; mRNA = messenger RNA; SYP = synaptophysin; ^{-/-} = without or with stable transfection of indicated vectors.

Fig. 8 and 9). When cells were cultured in fetal bovine serum medium, eight NEPC biomarkers were upregulated by SRRM4, the effects of which were enhanced by *RB1* or *TP53* depletion (Fig. 5a). SRRM4 in combination with loss of function of *RB1* or *TP53* showed a dramatically stronger propensity to upregulate NEPC biomarkers under ARPI. CHGB, NSE, SYP, and secretogranin III protein levels were enhanced by SRRM4 and further increased by ARPI and/or *RB1* or *TP53* knockdown (Fig. 5b). Nevertheless, *RB1* or *TP53* knockdown alone or in combination with ARPI did not significantly affect NEPC biomarker expression if SRRM4 was absent (Supplementary Fig. 8 and 9), suggesting that these two genes are facilitators of the NEPC phenotype. In summary, SRRM4 becomes a more potent driver of NEPC transdifferentiation under ARPI. Loss of function of *RB1* and *TP53* may facilitate this process.

3.7. SRRM4 alters the morphology of epithelial prostate cancer cells and establishes neuroendocrine prostate cancer xenografts

Under AR inhibition, LNCaP cells changed their epithelial spear morphology to compact cell bodies with extended fine branches but still grew as an adherent monolayer (Fig. 5c). Gain of SRRM4 led to formation of three-dimensional (3D) multicellular spheroids with strong SYP expression. The sizes and numbers of these spheroids were statistically greater in *TP53*-depleted cells (Fig. 5c). DHT reversed these morphologic changes and upregulation of NEPC biomarkers (Supplementary Fig. 10), indicating that the NEPC phenotype was not yet stably established at approximately 4 wk. Because *TP53* and *RB1* are cell cycle regulators, we cultured LNCaP cells in both two-dimensional (2D) and collagen-embedded 3D culture conditions to show that *TP53*, but not *RB1*, enhanced BrdU incorporation regardless of SRRM4 overexpression (Fig. 5d). Our colony formation assays further demonstrated that *RB1* and *TP53* can enhance anchorage-independent cell growth in the absence of SRRM4 (Fig. 5e). SRRM4 can also stimulate colony formation, supporting its role for NEPC progression. This SRRM4 function was strengthened by depletion of *TP53* but not *RB1*.

Current evidence suggests that AR inhibition, cyclic adenosine monophosphate (cAMP), or interleukin 6 can induce neuroendocrine transdifferentiation of LNCaP cells under 2D culture conditions; however, this is limited to upregulation of NEPC biomarkers [16–19]. No study has shown that LNCaP xenografts can be transformed into NEPC tumors after ARPI. When exogenous SRRM4 was introduced into LNCaP cells in the presence of *RB1* or *TP53* knockdown in castrated nude mice, SRRM4 established NEPC xenografts with strong SYP expression detected by both enzyme-linked immunosorbent assay on serum samples and by immunohistochemistry (Fig. 6). In SRRM4-established NEPC tumors, *TP53* depletion consistently showed enhanced NEPC transdifferentiation. Interestingly, these NEPC xenografts heterogeneously expressed the AR and prostate-specific antigen (PSA) (Fig. 6c). Indeed, many cells in SRRM4⁺/SYP⁺ tumors are AR and PSA negative, whereas all cells in SRRM4⁻/SYP⁻ xenografts are AR and PSA positive. These

results support the idea that SRRM4 drives transdifferentiation of AdPC to NEPC, accompanied by AR signaling being stochastically diminished.

4. Discussion

It is anticipated that NEPC will become more prevalent with widespread adoption of potent ARPI for CRPC. Consequently, better understanding of the molecular mechanisms by which NEPC develops is necessary to design therapeutic strategies for NEPC. Our finding that SRRM4 drives AdPC transdifferentiation to NEPC through AS of multiple genes including *REST* is novel. Importantly, ARPI in the context of *TP53* depletion exponentially escalates SRRM4-driven NEPC transdifferentiation. Our findings suggest that ARPI, genomic abnormality (eg, *TP53* and *RB1* genes), and reprogrammed transcription/AS programs (eg, by SRRM4 and *REST*) can combine to drive NEPC progression.

Consensus on the epidemiology of NEPC has not been reached [5]. Multiple hypotheses have been proposed including that NEPC originates from (1) adenocarcinoma cells through transdifferentiation, (2) clonal selection of pluripotent stem-like prostate epithelial cells, or (3) benign neuroendocrine cells. Accumulating evidence favors the first hypothesis. Genetic characterization of NEPC tumors [20,21] and PDXs [6] showed a high degree of similarity to their adenocarcinoma counterparts. Androgen depletion, cAMP, or cytokines can also stimulate adenocarcinoma cells to express NEPC biomarkers [16–19]. Although elevated SRRM4 expression was reported to be correlated with NEPC progression [22], we demonstrated for the first time that SRRM4 is a causal factor that not only can induce adenocarcinoma cells to express NEPC biomarkers but also can alter cellular morphology and, even more importantly, transform AdPC into NEPC xenografts in vivo. SRRM4 is a master regulator of neural-specific exon networks required for embryonic stem cells to transdifferentiate into neural cells [12,15]. Many SRRM4-targeted genes (eg, *REST* and *PHF21A*) in neural cells were also identified in NEPC, suggesting that SRRM4 is functionally active in NEPC [6,7]. It is noteworthy that several SRRM4 target genes are epigenetic histone modifiers, transcription factors, and RNA splicing factors. These findings indicate that SRRM4 can be a master regulator to reprogram AdPC transcriptomes into NEPC transcriptomes through AS alone. They highlight the importance of AS in determining tumor progression, something often overlooked in global transcriptome analyses.

Although SRRM4 regulates *REST* splicing, knockdown of *REST* does not affect SRRM4 expression, indicating that SRRM4 is an upstream regulator of *REST* in prostate cancer cells. As a global regulator, SRRM4 has much broader functions. Although *REST* knockdown stimulates NEPC biomarker expression, it does not alter LNCaP cell morphology and is not sufficient to establish NEPC xenografts, indicating that loss of function of *REST* is adequate to confer NEPC phenotype but not sufficient to induce NEPC transdifferentiation. Our results demonstrate that SRRM4 is a powerful driver of NEPC transdifferentiation.

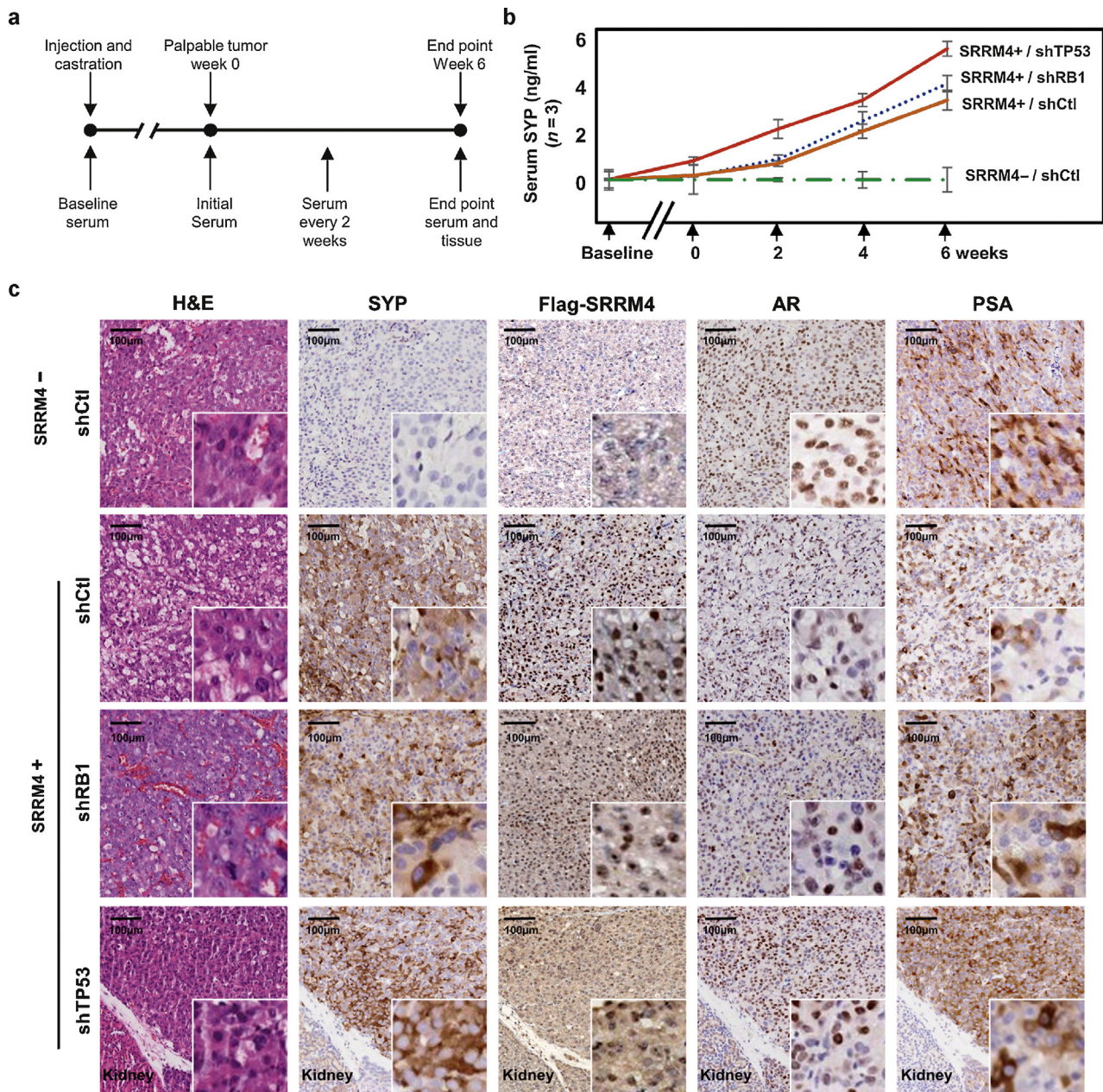


Fig. 6 – SRRM4 drives transdifferentiation of LNCaP xenografts to neuroendocrine prostate cancer tumors. (a) Schematic diagram shows the time points of serum collection from mice bearing LNCaP xenografts. (b) Serum SYP concentrations from mice bearing LNCaP(SRRM4⁻/shCtl), LNCaP(SRRM4⁺/shCtl), LNCaP(SRRM4⁺/shRB1), and LNCaP(SRRM4⁺/shTP53) xenografts (six grafts in three mice) were measured. Enzyme-linked immunosorbent assays were repeated in triplicate. (c) Immunohistochemistry was performed with indicated antibodies. Hematoxylin and eosin staining was also carried out. Scale bars = 100 μ m.

AR = androgen receptor; Ctl = control; H&E = hematoxylin and eosin; PSA = prostate-specific antigen; SYP = synaptophysin.

The prerequisite condition for SRRM4 to establish NEPC tumors is ARPI, since SRRM4 cannot cause morphologic changes in LNCaP cells and cannot induce NEPC xenografts when androgens are present. Our study also showed that enhanced SRRM4 expression and ARPI can block *REST* function through AS and protein degradation, respectively (Fig. 4) [10]. These findings explain interdependent and additive effects of SRRM4 and ARPI for NEPC progression.

Our results indicated that SRRM4 induction of the NEPC phenotype is enhanced by *RB1* or *TP53* depletion (Fig. 5).

When combined with ARPI, SRRM4 functions are further enhanced by *TP53* loss (Fig. 5 and 6). Based on these results and others, we propose a model of AdPC transdifferentiation to NEPC involving two types of gene regulators in two steps. The first type of genes including *AR*, *SRRM4*, and *REST* function as cell-differentiation regulators. They control epigenetics, transcription, and AS to confer an NEPC phenotype. ARPI releases AR-induced epithelium differentiation, thus providing an opportunity for cells to reset differentiation to NEPC. SRRM4 reprograms *REST* function

through AS and globally regulates neural-specific epigenetic histone modifiers, transcription factors/cofactors, and RNA splicing factors that are necessary for the NEPC phenotype. Nevertheless, this phenotypic transition cannot be detected until the transdifferentiated NEPC cells lock in their phenotypes. The second type of genes includes *TP53*, *RB1*, and *AURKA* cell cycle regulators. Genetic alterations of these genes facilitate NEPC transdifferentiation by bypassing cell cycle checkpoints. Cells bearing these genetic alterations also gain selective growth advantage under ARPI. This step is significant because it enriches NEPC cell numbers and biomarkers above a critical threshold allowing pathologic detection; however, loss of function of *RB1* or *TP53* likely does not play a direct role in NEPC transdifferentiation because these genes also exist in many AdPC tumors. Consistent with this, we showed that *TP53* or *RB1* depletion did not change NEPC biomarker expression (Supplementary Fig. 8 and 9). Consequently, genomic heterogeneity may predispose some prostate cancer cells to stably establish an NEPC phenotype once they transdifferentiate. This partially explains variations in NEPC marker expression in different prostate tumors [23].

The mechanisms of induction of *SRRM4* remain unknown. No NEPC-specific mutations were found in the *SRRM4* promoter, thus induction of *SRRM4* gene expression may involve epigenetic mechanisms involving histone post-translational modifications. Development of NEPC tumors is not rapid. The LTL331 PDX progressed to NEPC approximately 6 mo after castration [6]. It took 6 yr for the original tumor that gave rise to the LTL331 xenograft to recur in the patient as NEPC. Multiple temporal steps that include epigenetic modifications, including those involving *SRRM4*, may be required before the NEPC phenotype is stably established; however, such a hypothesis cannot fully explain why not all tumors or all cancer cells within a tumor eventually develop into NEPC. We hypothesize that some uncharacterized mutations in AdPC genomes may be prerequisite for and cooperate with *SRRM4*-regulated and other epigenetic changes for NEPC. These questions warrant further investigation.

5. Conclusions

We defined complex mechanisms by which *SRRM4* regulates AS programs to drive NEPC under ARPI.

Author contributions: Xuesen Dong had full access to all the data in the study and takes responsibility for the integrity of the data and the accuracy of the data analysis.

Study concept and design: Dong, Collins, YZ Wang.

Acquisition of data: Li, Donmez, Beltran.

Analysis and interpretation of data: Li, Donmez, Dong.

Drafting of the manuscript: Dong, Donmez.

Critical revision of the manuscript for important intellectual content: Gleave, YZ Wang, Collins.

Statistical analysis: Li, Donmez, Mo, Sahinalp.

Obtaining funding: Dong, YZ Wang, Sahinalp, Collins.

Administrative, technical, or material support: Xie, YW Wang, Xue.

Supervision: Dong, Collins.

Other (specify): None.

Financial disclosures: Xuesen Dong certifies that all conflicts of interest, including specific financial interests and relationships and affiliations relevant to the subject matter or materials discussed in the manuscript (eg, employment/ affiliation, grants or funding, consultancies, honoraria, stock ownership or options, expert testimony, royalties, or patents filed, received, or pending), are the following: None.

Funding/Support and role of the sponsor: This work was supported by an operating grant from the Canadian Institutes of Health Research (MOP-137007) and Prostate Cancer Canada (RS2013-58) to D.X. and by the Urology Foundation (charitable organization number 889494399) for the LAST project and by the BC Cancer Foundation (grant number DRG01518; ID: 1NSRG030) for W.Y.Z. and Genome Canada Grant (176ISO) for S.C. and C.C.

Acknowledgments: The authors acknowledge Rebeca Wu and Estelle Li for their technical support for pathology analyses.

Appendix A. Supplementary data

Supplementary data associated with this article can be found, in the online version, at <http://dx.doi.org/10.1016/j.eururo.2016.04.028>.

References

- [1] Scher HI, Fizazi K, Saad F, et al. Increased survival with enzalutamide in prostate cancer after chemotherapy. *N Engl J Med* 2012; 367:1187–97.
- [2] Hirano D, Okada Y, Minei S, Takimoto Y, Nemoto N. Neuroendocrine differentiation in hormone refractory prostate cancer following androgen deprivation therapy. *Eur Urol* 2004;45:586–92, discussion 592.
- [3] Sasaki T, Komiya A, Suzuki H, et al. Changes in chromogranin a serum levels during endocrine therapy in metastatic prostate cancer patients. *Eur Urol* 2005;48:224–30, discussion 229–30.
- [4] Beltran H, Rickman DS, Park K, et al. Molecular characterization of neuroendocrine prostate cancer and identification of new drug targets. *Cancer Discov* 2011;1:487–95.
- [5] Terry S, Beltran H. The many faces of neuroendocrine differentiation in prostate cancer progression. *Front Oncol* 2014;4:60.
- [6] Lin D, Wyatt AW, Xue H, et al. High fidelity patient-derived xenografts for accelerating prostate cancer discovery and drug development. *Cancer Res* 2014;74:1272–83.
- [7] Lapuk AV, Wu C, Wyatt AW, et al. From sequence to molecular pathology, and a mechanism driving the neuroendocrine phenotype in prostate cancer. *J Pathol* 2012;227:286–97.
- [8] Akamatsu S, Wyatt AW, Lin D, et al. The placental gene PEG10 promotes progression of neuroendocrine prostate cancer. *Cell Rep* 2015;12:922–36.
- [9] Tan HL, Sood A, Rahimi HA, et al. Rb loss is characteristic of prostatic small cell neuroendocrine carcinoma. *Clin Cancer Res* 2014;20: 890–903.
- [10] Svensson C, Ceder J, Iglesias-Gato D, et al. REST mediates androgen receptor actions on gene repression and predicts early recurrence of prostate cancer. *Nucleic Acids Res* 2014;42:999–1015.
- [11] Gopalakrishnan V. REST and the RESTless: in stem cells and beyond. *Future Neurol* 2009;4:317–29.
- [12] Raj B, Irimia M, Braunschweig U, et al. A global regulatory mechanism for activating an exon network required for neurogenesis. *Mol Cell* 2014;56:90–103.

- [13] Mosquera JM, Beltran H, Park K, et al. Concurrent AURKA and MYCN gene amplifications are harbingers of lethal treatment-related neuroendocrine prostate cancer. *Neoplasia* 2013;15: 1–10.
- [14] Nakano Y, Jahan I, Bonde G, et al. A mutation in the Srrm4 gene causes alternative splicing defects and deafness in the Bronx waltzer mouse. *PLoS Genet* 2012;8:e1002966.
- [15] Calarco JA, Superina S, O'Hanlon D, et al. Regulation of vertebrate nervous system alternative splicing and development by an SR-related protein. *Cell* 2009;138:898–910.
- [16] Bang YJ, Pirnia F, Fang WG, et al. Terminal neuroendocrine differentiation of human prostate carcinoma cells in response to increased intracellular cyclic AMP. *Proc Natl Acad Sci U S A* 1994; 91:5330–4.
- [17] Shen R, Dorai T, Szaboles M, Katz AE, Olsson CA, Buttyan R. Trans-differentiation of cultured human prostate cancer cells to a neuroendocrine cell phenotype in a hormone-depleted medium. *Urol Oncol* 1997;3:67–75.
- [18] Zhu Y, Liu C, Cui Y, Nadiminty N, Lou W, Gao AC. Interleukin-6 induces neuroendocrine differentiation (NED) through suppression of RE-1 silencing transcription factor (REST). *Prostate* 2014;74: 1086–94.
- [19] Cortes MA, Cariaga-Martinez AE, Lobo MV, et al. EGF promotes neuroendocrine-like differentiation of prostate cancer cells in the presence of LY294002 through increased ErbB2 expression independent of the phosphatidylinositol 3-kinase-AKT pathway. *Carcinogenesis* 2012;33:1169–77.
- [20] Sauer CG, Roemer A, Grobholz R. Genetic analysis of neuroendocrine tumor cells in prostatic carcinoma. *Prostate* 2006;66:227–34.
- [21] Lotan TL, Gupta NS, Wang W, et al. ERG gene rearrangements are common in prostatic small cell carcinomas. *Mod Pathol* 2011;24: 820–8.
- [22] Zhang X, Coleman IM, Brown LG, et al. SRRM4 expression and the loss of REST activity may promote the emergence of the neuroendocrine phenotype in castration-resistant prostate cancer. *Clin Cancer Res* 2015;21:4698–708.
- [23] Mucci NR, Akdas G, Manely S, Rubin MA. Neuroendocrine expression in metastatic prostate cancer: evaluation of high throughput tissue microarrays to detect heterogeneous protein expression. *Hum Pathol* 2000;31:406–14.

www.eurep17.org

EUREP17

15th European Urology Residents
Education Programme

1-6 September 2017, Prague, Czech Republic



eau esu European School of Urology